Dear Editor:

We are grateful for the reviewers and your efforts and time to improve our manuscript. In this version, we have made revisions as suggested by you and the two reviewers. Please find our materials in sequence as follow:

(1) We have answered the new three questions from the reviewers in the **Text 1**;

(2) We have strengthened the coherence of this article and made it more readable. The detailed information about the three-pool model has been provided in the main text as section 2.3 (*Methods*, 618 words) and 3.3 (*Results*, 193 words).

(3) The former response letter has been updated with the new results and is shown in **Text 2**.

Text 1

Comment 1C: *Please justify your use of the entirely new three-pool model, when there are a range of existing Community Land Models available?*

Response: The authors thank the reviewer for this suggestion. We have explained the reasons for selecting this three-pool model in the *Method* section of this revised version. We also have highlighted the existence of multiple model structures and recommend a biogeochemical model database in the discussion of the methodological uncertainty of this study. Please find our revisions in detail as below:

The selection of three-pool model: As mentioned by the reviewer, there is a range of existing Community Land Models (CLM) available. The Fig. R1.1 shows the structures of soil carbon model in the CENTURY model and the two recent versions of CLM. The latest version CLM (i.e., CLM5.0) used the same three-pool structure as CENTURY (panel a) and CLM4.5 (panel c). Many other global land models adopted the structure of CENTURY model due to its success of capturing the soil carbon dynamics over inter-annual to decadal timescales (Parton *et al.*, 1993; Luo *et al.*, 2015). Thus, we selected this three-pool model structure in our analysis (please see more on our reply to "Comment 1B").

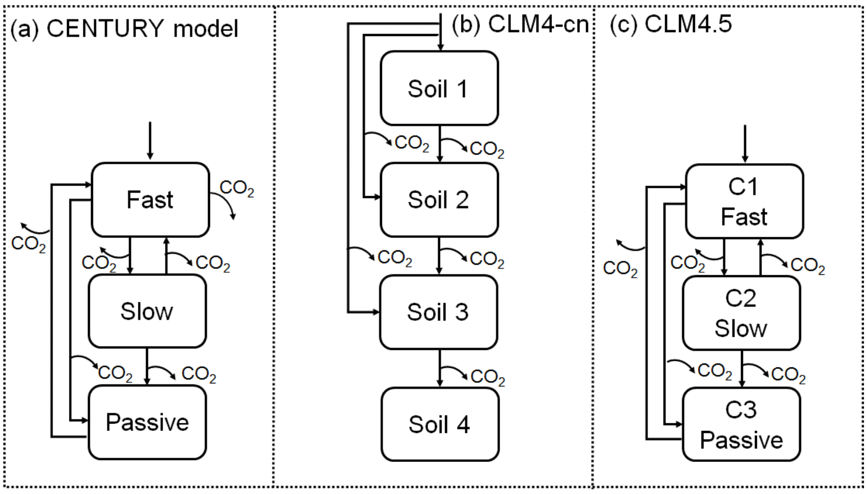

Figure R1.1 The soil carbon model structures of the CENTRY, CLM-cn and CLM4.5 models.

Highlight of the uncertainty from model structure: Multicompartment models have been widely used to study soil carbon dynamics in current Earth system models (Manzoni and Porporato 2009; Sierra et al., 2015, 2018). For example, the terrestrial component of the HadGEM2 model (i.e., JUELS) uses a four-pool model to evaluate the soil organic (Collins et al., 2011). The MPI-ESM model represents the soil carbon stocks as two compartments (Roeckner et al., 2011). As shown in the Fig. R1.1, the CLM4-cn and CLM4.5 models differ in their structures of soil carbon component, but they both represent the soil organic carbon pool as multiple compartments (Lawrence et al., 2011; Oleson et al., 2013). The various structures of these soil carbon-cycle models have been nicely summarized into a "biogeochemical model database (bgc_md)" by the Theoretical Ecosystem Ecology Group in Max Planck Institute for Biogeochemistry (https://github.com/MPIBGC-TEE/bgc-md). Such effort is very important for evaluating the structure uncertainty in the estimates of soil C transit time. In this version, we have highlighted this point and cited the "bgc_md" as a supplementary for the readers (Line 19-24, Page 12):

> "As synthesized by Sierra et al. (2017), the observations of τ_{soil} are useful for a specific model once its pool structure is identified. This study also detect difference in the estimated τ_{soil} between the one- and three-pool models (Fig. 4). Thus, model database, such as the bgc-md (https://github.com/MPIBGC-TEE/bgc-md), could be a useful tool to improve the integration of observations and soil C models."

Comment 2C: *In your response to reviewer 2, please provide more detail on the new approach. What would drive soil C input? Would the model be calibrated against data from all sites?*

Response: Thanks. We have revised our responses to reviewer 2 with more detail on the new approach in this version. In brief, we assumed the total soil carbon input equals to total soil respiration at the steady state (Line 12-13, Page 6). The total C stocks and CO_2 efflux from observations were separated into pool-specific decomposition rates by deconvolution analysis (Fig.R1.1a, Liang et al., 2015). Although there are some parameters could not well-constrained, all the model would be calibrated against data (Table R1.1 and Fig. R2). The transit time of each biome were simulated with the equation (7) in our reply to Comment 2B.

Table R1.1 Maximum likelihod estimates of parameters, *P*-value, R^2 and the Akaike information criterion (*AIC*) values in the three-pool model with observations.

Biomes	Q_{10}			Transit time (year)				*P*	R^2	*AIC*
	fast	slow	passive	fast	slow	passive	Mean			
Boreal forest	1.4	2.8	3.1	4.7	84.2	131.8	66.4	< 0.05	0.95	-158.9
Temperate forest	2.2	1.4	0.8	3.2	28.8	36.8	79	< 0.05	0.96	-167.5
Tropical forest	2.5	1.1	1.4	3	18.7	18.9	28.9	< 0.05	0.95	-224.7
Cropland	2.3	1.3	1.6	3.2	34.5	71.1	77.1	< 0.05	0.99	-209.5
Tundra	2.9	4.2	3.8	47.1	54.9	105.8	166.5	< 0.05	0.96	-106.1
Desert/Shrubland	2.5	1.3	3.7	32.7	55.8	114.8	135.3	< 0.05	0.95	-88.5
Grassland/Savanna	1.9	1.1	2.8	22.6	45.9	88.3	53.8	< 0.05	0.95	-45.8

In total, five out of eleven parameters were constrained for tundra ecosystem (Fig. S1). Eight out of eleven parameters were constrained for temperate, boreal forest and desert & shrubland (Fig. S2, S3, S6). Seven out of eleven parameters were constrained for tropical forest and cropland (Fig. S4, S5). For grassland and savanna, seven out of eleven parameters were constrained (Fig. S7).

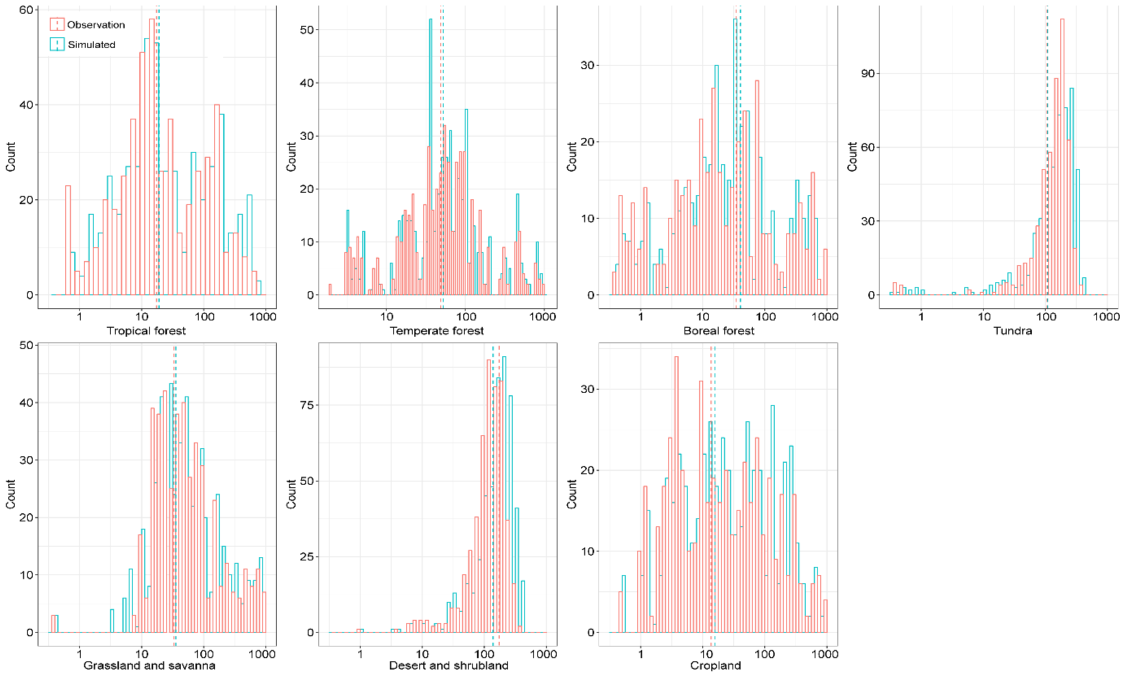

Figure R1.2. The histogram of SOC transit time (τ_{soil}) from observational data and simulation based on data assimilation analysis. The dash line indicates the median of the τ_{soil}.

Comment 3C: *It is difficult to follow how transit time from the same Q10-based first-order kinetics model would be so insensitive to temperature (see Fig R2.1 in the supplement to their replies to my comments).*

Response: Sorry for confusion. The Fig. R2.1 shown the SOC τ_{soil} based on the observational data and CLM5 models results at the steady state, respectively. The transit times of 12 CMIP5 models were calculated by averaging τ_{soil} of each model. For each model, the τ_{soil} divided the SOC and NPP. Thus, the small SOC and NPP generated the small τ_{soil} in this study.

<u>Text 2</u>

Responses to Reviewer A

Comment 1A: *In this paper, the authors evaluate soil carbon transit times in 12 CMIP5 models. They found that, compared to in-situ observations, transit times are usually underestimated by models, especially in cold regions and dry/hot regions. The authors show that some of these biases can be resolved by adopting more vertically-resolved parameterization of soil C dynamics with the CLM4.5 model.*

Response: Thanks for the clear summary of our manuscript.

Comment 2A: *I have concerns about this manuscript as it seems very similar to previous papers by e.g. Todd-Brown et al. (2013): the same models are evaluated with the same HWSD-MODIS based product. The novelty here is the comparison of models against transit times measured in worldwide soils, and I think it should be the main aim of the study. If the authors decide to keep the global evaluation, the HWSD-MODIS product should be confronted to in situ observations to justify its use as a global benchmark or, alternatively, the creation of this database could be used to derive a more robust global product.*

Response: We agree that Todd-Brown *et al.*, (2013) was the first study which has done the wonderful evaluation on the large uncertainty of soil C turnover time based on the HWSD-MODIS products and 12 CMIPS models. As pointed out by the reviewer, the unique contribution of our study is using the *in-situ* observations to benchmark the global models. In order to avoid the confusion, we have removed the results based on HWSD-MODIS products (i.e., the original panels c and d in the Fig. 3) in the revised version. Please see the updated Fig. 3 as below:

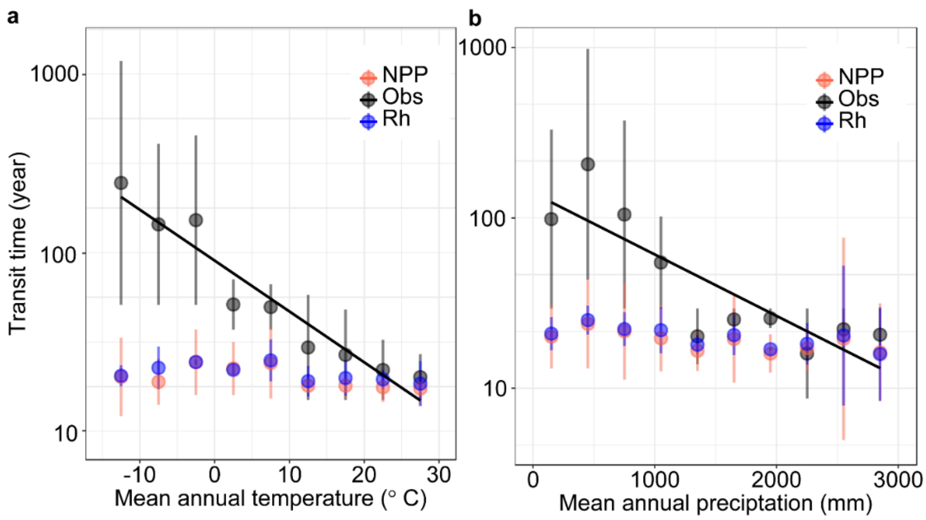

Figure R 2.1 Relationships between SOC transit time (τ_{soil}) and climate factors in both observations and CIMP5 models. The black solid lines show the negative correlation between τ_{soil} and (**a**) mean annual temperature and (**b**) mean annual precipitation. The black dots indicate the aggregated τ_{soil} over each category of MAT (y= -5.47x+1971.5, r^2 = 0.49, P<0.01) or MAP (y= -68.19x+1222.6, r^2 = 0.60, P<0.01). The red and blue dots present the mean value of the multiple models based on the ratios of carbon stock over NPP and R_h, respectively.

Comment 3A: *Section 3.2 is very hard to understand. It is not clear whether models are evaluated against the in-situ observations, or whether they are evaluated against the HWSDMODIS based global product (as it seems in Fig. 3). The discussion around improvements due to the addition of a vertical resolution in CLM4.5 is reduced to less than 10 lines while it seems to be one of the key findings of the whole study.*

Response: The Section 3.2 is mainly the evaluation of models against the *in-situ* observations. In this version, we have made this section clearer by:

(1) We have added more details about the comparison between model results and the in-situ observations. In brief, only the grid cells containing the locations of in-situ observations were selected from the models for the comparison.
(2) To avoid confusion, we have removed the HWSD/MODIS results in this version.
(3) The results based on the vertical resolution in CLM4.5 have be expanded in the section 3.4.

Specific Comments:

Comment 4A: *p3 l 21-29: which period of the historical simulation did the authors consider?*

Response: The historical period is from 1850 to 1860. We have made it clear in the revision.

Comment 5A: *p3 l30: I find that there is a missed opportunity here to use in situ observations to derive a more robust global dataset of transit times. HWSD and MODIS NPP both come with known biases and there may be other products to choose from e.g. soilgrids (www.soilgrids.org).*

Response: As mentioned above, we will remove the results based on HWSD and MODIS in the revised version. We thank the reviewer for the suggestion of deriving a robust global dataset of transit time based on the observations. This task is scientifically very important, but is difficult at the current stage due to a few reasons. First, the available observations are limited by the unequal quality and the uneven spatial distribution of the locations. Second, no data-driven approach is ready for deriving a global dataset of C transit time based on the observations. Third, it is difficult to reduce the methodological uncertainty of data (e.g., Fig. 1b) in integrating them into a given model for global calculation. We will discuss this issue in the revised manuscript.

Comment 6A: *p6 l30-35: I do not understand what is learned by replacing MODIS NPP with TRENDY models (which ones? reference is missing here). Does that mean that TRENDY is considered as an observation of NPP against which ESMs are evaluated?*

Response: The results from TRENDY and MODIS NPP have been removed in this version. Also, we agree with the reviewer that TRENDY NPP cannot used as observations.

Comment 7A *Figure 2: from the legend, panels c and d are missing. Panel a is hard to understand and uncertainties are missing from panel b.*

Response: Sorry for the confusion. We have corrected the figure legend in the revised version. More sentences will be added to explain the panel a, and the uncertainties have been added in the panel b.

Comment 8A *Figure 3: in panel a and b, do black dots represent data from the 187 sites? or were they extracted from the HWSD/MODIS product?*

Response: The black dots represent data from 187 sites in panel (a) and (b) in Fig. 3, we grouped them into different levels of climatic variables. We will revise the figure legend to make it clearer. Also, the panels *c* and *d* will be removed to avoid confusion.

Review B:

Comment 1B: *In this manuscript, the authors present observation-based estimates of transit times of carbon in soils and compare these estimates with model predictions. This is an important topic because transit times are a very good constraint for evaluating model performance. There has been a lot of recent research on this topic, motivated in part by the work of Carvalhais et al. (2014), who used a stock-over-flux approach to compute residence times from models and observations. Recent publications have shown that this approach has problems to compute transit times for systems of multiple pools and out of equilibrium (Lu et al., 2018; Sierra et al., 2017), and better methods for estimating transit times for systems out of equilibrium have been developed (e.g. Rasmussen et al., 2016).*

Response: We thank the reviewer for the great summary. We have revise the introduction of our manuscript to highlight these milestone works as mentioned by the reviewer.

Major remark:

Comment 2B: *Despite these recent developments, this manuscript uses observations from incubation experiments and ^{13}C measurements from C_3/C_4 vegetation replacement experiments, in which the rate of soil carbon loss is estimated assuming one single pool in equilibrium. This is evidenced by equations (1) to (3) in Text S1 of the supplementary material. The implication of this assumption is that the observations are treated as a homogeneous system, without differentiating between the age of the stored carbon and the age of the carbon in the efflux. In the introductory paragraphs, the manuscript gives the impression that it provides an advance by providing observation estimates of transit times, but in reality, these estimates suffer the same problems of previous approaches.*

I recommend the authors to use the data they compiled to fit multiple-pool models to better estimate age and transit times from these observations. You probably would still need to keep the steady-state assumption for this type of observations, but at least you can remove the one-single homogeneous pool assumption.

Response: Many thanks for thoughtful suggestion. We have followed the reviewer's suggestion to fit the data to a three-pool model in addition to the single pool approach. Then, we estimated the C transit time from the observations under the steady-state assumption. The reasons for the selection of the three-pool model has been summarized in our above reply to the "Comment 1C". As shown in the Fig. R2.3, there are differences in the estimated τ_{soil} between the one- and three-pool models. However, the underestimation of τ_{soil} by the CMIP5 models were detected by both of one- and three-pool models. The estimated parameters and new results could be found in the Table R1.1and Table 2.1. Please also find the details of the three-pool model as below:

The dynamics of SOC are widely represented by models with multiple pools. For the better estimation of the carbon transit times, we fitted a three-pool model with the observational data derived from stock-over-flux approach. In this study, a three-pool C model consisted of fast, slow, and passive pools and carbon transfers among three pools (Fig. R2.2). This model shares the same framework with the CENTURY and the CLM4.5 (Fig. R1.1). The dynamics of soil carbon pools follow the first-order differential kinetics. Based on the theoretical analysis, the C dynamics of the three-pool model can be mathematically described by the following matrix equation (Luo *et al*., 2003; Xia *et al*., 2013) as:

$$\frac{dC(t)}{dt} = I(t) - AKC(t) \tag{1}$$

where the matrix $C(t) = (C_1(t), C_2(t), C_3(t))^T$ is used to describe soil carbon pool sizes. A is a matrix given by:

$$A = \begin{pmatrix} -1 & f_{12} & f_{13} \\ f_{21} & -1 & 0 \\ f_{31} & f_{32} & -1 \end{pmatrix} \tag{2}$$

The elements f_{ij} are carbon transfer coefficients, indicating the fractions of the C entering *i*-th (row) pool from *j*-th (column) pool. K is a 3×3 diagonal matrix indicating the decomposition rates (the amounts of C per unit mass leaving each of the pools per year). The matrix of K is given by: $K = \text{diag}(k_1, k_2, k_3)$. The total C stocks and CO_2 efflux from observations were separated into pool-specific decomposition rates by deconvolution analysis (Fig. R2.2, Liang et al., 2015). At the steady state, the total soil respiration equals to the total carbon input.

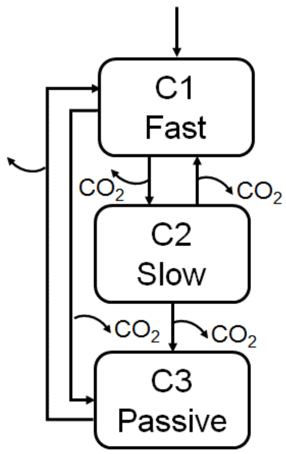

Figure R2.2 The diagram of three-pool model in this analysis.

The parameters in the three-pool model were estimated based on Bayesian probabilistic inversion (equation (4)). The posterior probability density function $P(\theta|Z)$ of model parameters (θ) can be represented by the prior probability density function ($P(\theta)$) and a likelihood function ($P(Z|\theta)$) (Liang *et al.*, 2015; Xu *et al.*, 2016). The likelihood function was calculated by the minimum error between observed and modelled values with equation (5). In this study, we adopted the prior ranges of model parameter from Liang et al. (2015).

$$P(\theta|Z) \propto P(Z|\theta)\cdot P(\theta) \quad (3)$$

$$P(Z|\theta) \propto \exp\left\{-\frac{1}{2\sigma_i^2(t)}\sum_{i=1}^{n}\sum_{t\in obs(Z)}[Z_i(t)-X_i(t)]^2\right\} \quad (4)$$

where $Z_i(t)$ and $X_i(t)$ are the observed and modelled transit times, and the $\sigma_i^2(t)$ is the standard deviation of measurements. The posterior probability density function of the parameters was constructed with two steps: a proposing step and a moving step. In the first step, the dataset was generated based on the previously accepted data with a proposal distribution:

$$\theta^{new}=\theta^{new}+\frac{d(\theta_{max}-\theta_{min})}{D} \quad (5)$$

where θ_{max} and θ_{min} are the maximum and minimum values of the given parameters, d is the random variable between -0.5 and 0.5 with uniform distribution, D is used to control the proposing step size in this study. In the moving step, the new data θ^{new} is tested against the Metropolis criteria to quantify whether it should be accepted or rejected. The parameters of posterior probability density function were constructed by the Metropolis-Hasting algorithm. The Metropolis-Hasting algorithm was run 50,000 times for observed data. Accepted parameter values were used in the further analysis.

Table R2.1. Prior parameters of three-pool simulation.

Parameter	Definition	Value	Range
Q_{10}	The temperature scalar in fast, slow and passive carbon pools	2	(0, 6)
f_{12}	The fraction of carbon from pool 2 to pool 1	0.1	(0.1, 0.6)
f_{13}	The fraction of carbon from pool 3 to pool 1	0.2	(0, 1)
f_{21}	The fraction of carbon from pool 1 to pool 2	0.5	(0.1, 0.6)
f_{31}	The fraction of carbon from pool 1 to pool 3	0.004	(0, 0.1)
f_{32}	The fraction of carbon from pool 2 to pool 3	0.03	(0, 0.03)
k_1	The decomposition rate of the fast soil carbon pool	0.01	(0.001, 0.05)
k_2	The decomposition rate of the slow soil carbon pool	0.006	(0.001, 0.0021)
k_3	The decomposition rate of the passive soil carbon pool	0.00002	(1.910^{-6}, $2.1\ 10^{-5}$)

Based on the concepts of mean age and mean transit time published by Rasmussen et al., (2016) and Lu et al., (2018), the mean carbon age defined as the whole time periods the carbon atoms stored in the carbon pools, and then the mean age of carbon $\bar{a}_i(t)$ in a certain carbon pool i could be calculated with equation (6):

$$\bar{a}_i(t)=1+\frac{\sum_{i=1}^{3}(\bar{a}_j(t)-\bar{a}_j(t))\cdot f_{ij}(t)\cdot C_i-\bar{a}_j(t)\cdot I_i(t)}{C_i} \quad (6)$$

where the $f_{ij}(t)$ are the carbon fraction transfer coefficients from *j*-th to *i*-th pools, $I_i(t)$ is the external input into the *i*-th carbon pool.

The transit time $\tau_i(t)$ was defined as the mean age of carbon atoms leaving the carbon pool at a specific time:

$$\tau_i(t)=\sum_{i=1}^{d} f_i(t)\cdot a_i(t) \quad (7)$$

where the $f_i(t)$ is the fraction of carbon with mean age $a_i(t)$.

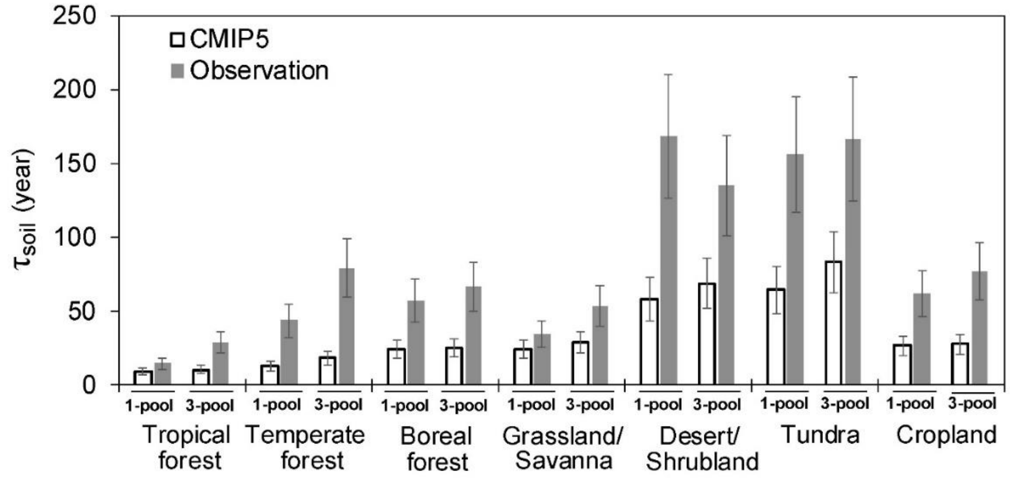

Figure R2.3 The SOC transit time (τ_{soil}) calculated from the one- and three-pool models under the steady-state assumption.

Comment 3B: *For a fair comparison with the model output, I recommend you compute their transit time at the spin-up state, which better represent the equilibrium state of the model. In the current version, you compute model-derived transit times from a multi-year average, but this corresponds to a transient state where transit times are not unique.*

Response: Thanks for the great suggestion. We have additionally analyzed the modeled C transit time over 1850-1860, when the models were close to the steady state. Using the modeled data over 1850-1860 and 1995-2005 (the original results) both have pros and cons. For example, the estimated C transit time based on 1850-1860 results holds the equilibrium assumption but neglect the changes of C transit time over time (i.e., the observations are from the recent decades). The original results (i.e., over 1995-2005) were not derived from the equilibrium state, but they catch the time period of the observations. However, the results were consistent by using the modelled data over 1850-1860 and 1995-2005.

Comment 4B: *Another aspect that requires clarification is the computation of the transit time distributions in Figure 1b. How were these distributions obtained from the data? Did you assume a specific distribution function and fitted its parameter values using the data? This seems to be the case for the 13 and the stock/flux data, but not for the incubations. Please clarify.*

Response: The Gaussian kernel density estimation (KDE) was used to obtain the distributions in the Figure 1b. The ^{13}C, stock/flux data and incubations both are follow the Gaussian kernel density distributions. The τ_{soil} from laboratory studies was significantly shorter than the other two methods, therefore they shared the different axis in Fig. 1b. The left axis is for ^{13}C and *stock-over-flux* approaches, and the right axis is for laboratory incubation studies. We have added illustration distribution function and detailed information in section 2.4 (*Statistical analysis*, Line 3-11, Page 10) as follow:

The Gaussian kernel density estimation (KDE) was used to obtain the distributions of observed transit times (Sheather & Marron, 1990; Saoudi *et al.*, 1997). The KDE is a non-parametric approach to estimate the probability density function of a random variable. Let $(x_1, x_2, \cdots, x_n)$ denote the observed SOC τ_{soil} with density function f as below:

$$\hat{f}_h(x) = \frac{1}{nh} \sum_{i=1}^{n} K\left(\frac{x-x_i}{h}\right) \tag{8}$$

where K is the non-negative density function than integrates to one and has mean zero, and $h > 0$ is a smoothing parameter called the bandwidth. The bandwidth for approaches of stable isotope ^{13}C, *stock-over-flux* and incubation are: 48.61, 35.13, 2.62, respectively.

References from reviewer A:

Todd-Brown, K.E., Randerson, J.T., Post, W.M., Hoffman, F.M., Tarnocai, C., Schuur, E.A. and Allison, S.D.: Causes of variation in soil carbon simulations from CMIP5 Earth system models and comparison with observations. Biogeosciences, 10, 1717-1736, https://doi: 10.5194/bg-10-1717-2013.

References from reviewer B:

Carvalhais, N., Forkel, M., Khomik, M., Bellarby, J., Jung, M., Migliavacca, M., Mu, M., Saatchi, S., Santoro, M., Thurner, M., et al. (2014). Global covariation of carbon turnover times with climate in terrestrial ecosystems. Nature, 514(7521):213.

Lu, X., Wang, Y.-P., Luo, Y., and Jiang, L. (2018). Ecosystem carbon transit versus turnover times in response to climate warming and rising atmospheric CO2 concentration. Biogeosciences Discussions, 2018:1–22.

Rasmussen, M., Hastings, A., Smith, M. J., Agusto, F. B., Chen-Charpentier, B. M., Hoffman, F. M., Jiang, J., Todd-Brown, K. E. O., Wang, Y., Wang, Y.-P., and Luo, Y. (2016). Transit times and mean ages for nonautonomous and autonomous compartmental systems. Journal of Mathematical Biology, 73(6):1379–1398.

Sierra, C. A., Müller, M., Metzler, H., Manzoni, S., and Trumbore, S. E. (2017). The muddle of ages, turnover, transit, and residence times in the carbon cycle. Global Change Biology, 23(5):1763–1773.

References from author

Bolker, B.M., Pacala, S.W. & Parton Jr, W.J. (1998) Linear analysis of soil decomposition: insights from the century model. *Ecological Applications*, **8**, 425-439.

Collins, W. J., Bellouin, N., Doutriaux-Boucher, M., Gedney, N., Halloran, P., Hinton, T., ... & Martin, G. (2011). Development and evaluation of an Earth-System model–HadGEM2. Geoscientific Model Development, 4(4), 1051-1075.

Lawrence, D. M., Oleson, K. W., Flanner, M. G., Thornton, P. E., Swenson, S. C., Lawrence, P. J., ... & Bonan, G. B. (2011). Parameterization improvements and functional and structural advances in version 4 of the Community Land Model. Journal of Advances in Modeling Earth Systems, 3(1).

Liang, J., Li, D., Shi, Z., Tiedje, J.M., Zhou, J., Schuur, E.A.G., Konstantinidis, K.T. & Luo, Y. (2015) Methods for estimating temperature sensitivity of soil organic matter based on incubation data: A comparative evaluation. *Soil Biology and Biochemistry*, **80**, 127-135.

Luo, Y., Gerten, D., Le Maire, G., Parton, W. J., Weng, E., Zhou, X., ... & Dukes, J. S. (2008). Modeled interactive effects of precipitation, temperature, and [CO2] on ecosystem carbon and water dynamics in different climatic zones. Global Change Biology, 14(9), 1986-1999.

Luo, Y., & Weng, E. (2011). Dynamic disequilibrium of the terrestrial carbon cycle under global change. Trends in Ecology & Evolution, 26(2), 96-104.

Luo, Y., Shi, Z., Lu, X., Xia, J., Liang, J., Jiang, J., ... & Chen, B. (2017). Transient dynamics of terrestrial carbon storage: mathematical foundation and its applications.

Manzoni, S., & Porporato, A. (2009). Soil carbon and nitrogen mineralization: theory and models across scales. Soil Biology and Biochemistry, 41(7), 1355-1379.

Oleson, K. W., Lawrence, D. M., Gordon, B., Flanner, M. G., Kluzek, E., Peter, J., ... & Heald, C. L. (2010). Technical description of version 4.0 of the Community Land Model (CLM).

Parton, W. J., Schimel, D. S., Cole, C. V., & Ojima, D. S. (1987). Analysis of factors controlling soil organic matter levels in Great Plains Grasslands 1. Soil Science Society of America Journal, 51(5), 1173-1179.

Rasmussen, M., Hastings, A., Smith, M.J., Agusto, F.B., Chen-Charpentier, B.M., Hoffman, F.M., Jiang, J., Todd-Brown, K.E., Wang, Y., Wang, Y.P. & Luo, Y. (2016) Transit times and mean ages for nonautonomous and autonomous compartmental systems. *J Math Biol*, **73**, 1379-1398.

Roeckner, E., Giorgetta, M. A., Crueger, T., Esch, M., & Pongratz, J. (2011). Historical and future anthropogenic emission pathways derived from coupled climate–carbon cycle simulations. *Climatic Change*, **105**, 91-108.

Saoudi, S., Ghorbel, F. & Hillion, A. (1997) Some statistical properties of the kernel - diffeomorphism estimator. *Applied stochastic models and data analysis*, **13**, 39-58.

Sheather, S.J. & Marron, J.S. (1990) Kernel quantile estimators. *Journal of the American Statistical Association*, **85**, 410-416.

Xu, X., Shi, Z., Li, D., Rey, A., Ruan, H., Craine, J.M., Liang, J., Zhou, J. & Luo, Y. (2016) Soil properties control decomposition of soil organic carbon: Results from data-assimilation analysis. *Geoderma*, **262**, 235-242.

Sierra, C. A., Harmon, M. E., & Perakis, S. S. (2011). Decomposition of heterogeneous organic matter and its long - term stabilization in soils. Ecological Monographs, **81**, 619-634.

Sierra, C. A., & Müller, M. (2015). A general mathematical framework for representing soil organic matter dynamics. Ecological Monographs, **85**, 505-524.

Supplementary figures:

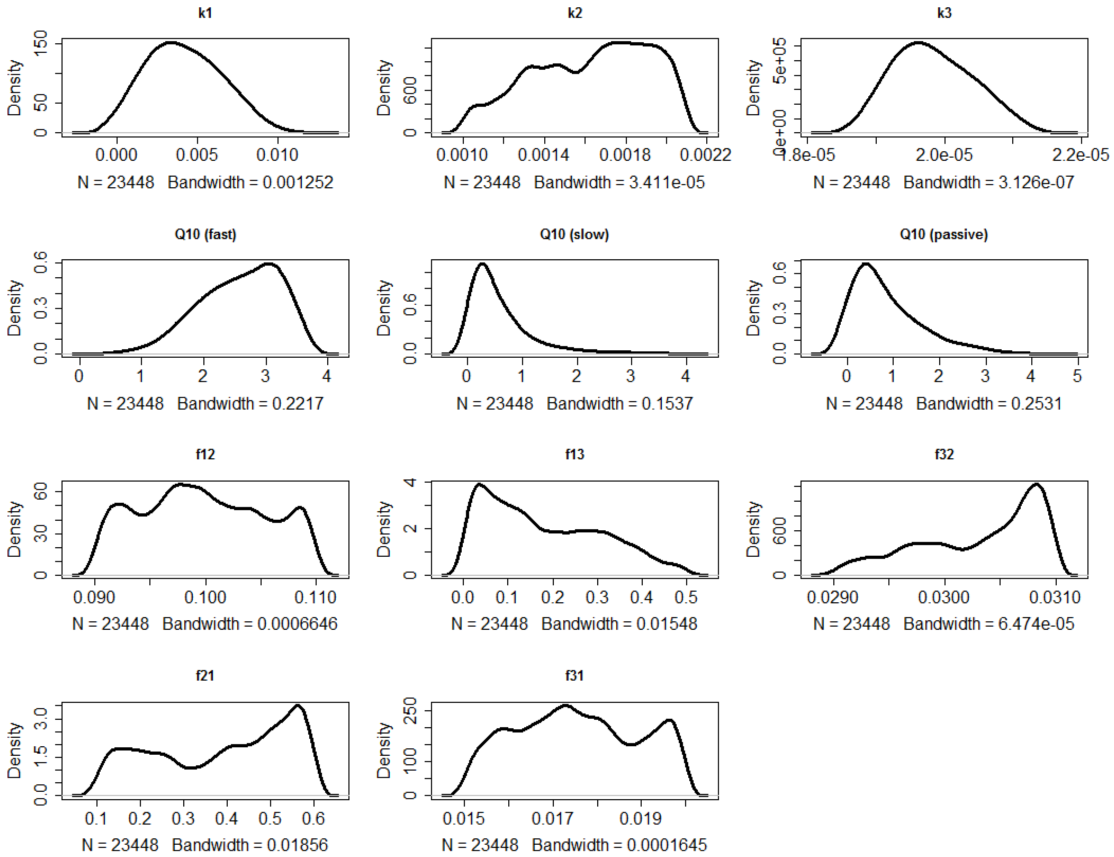

Figure S1. Probability distributions of the parameters in the three-pool model for tundra ecosystem (See Equation (1) for abbreviations).

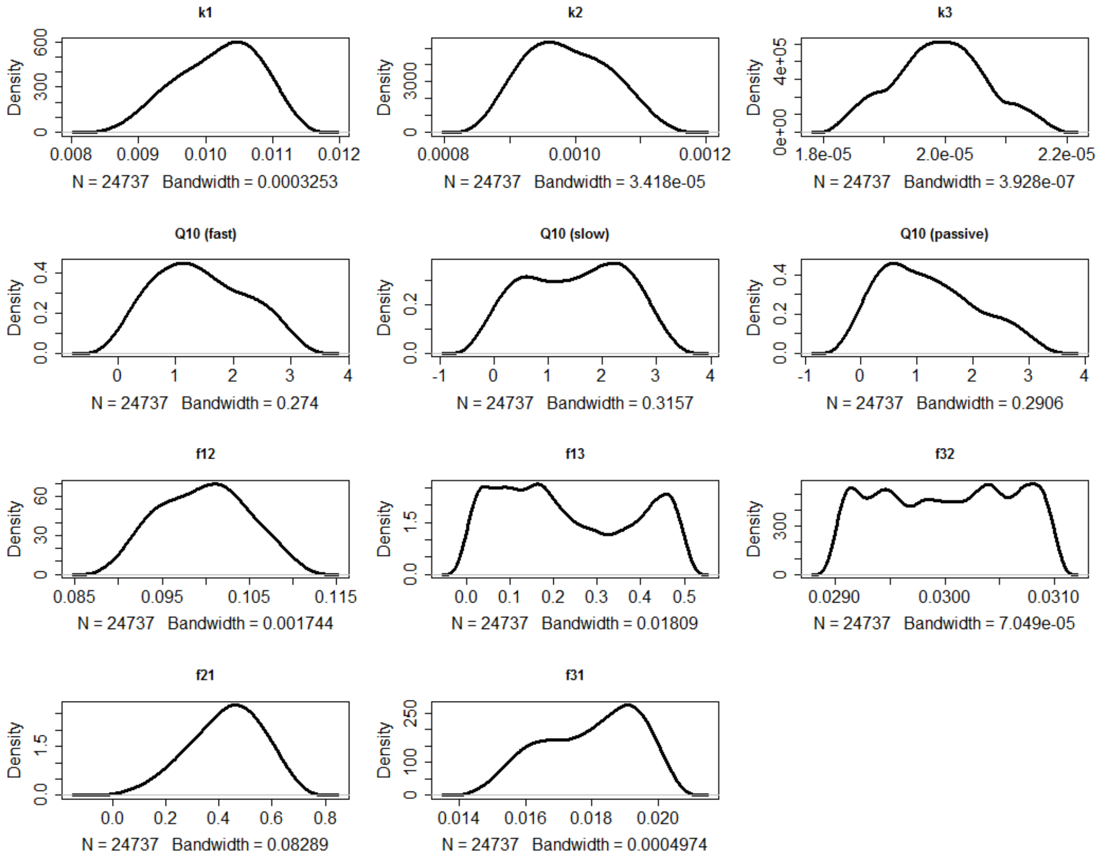

Figure S2. Probability distributions of the parameters in the three-pool model for boreal forest ecosystem (See Equation (1) for abbreviations).

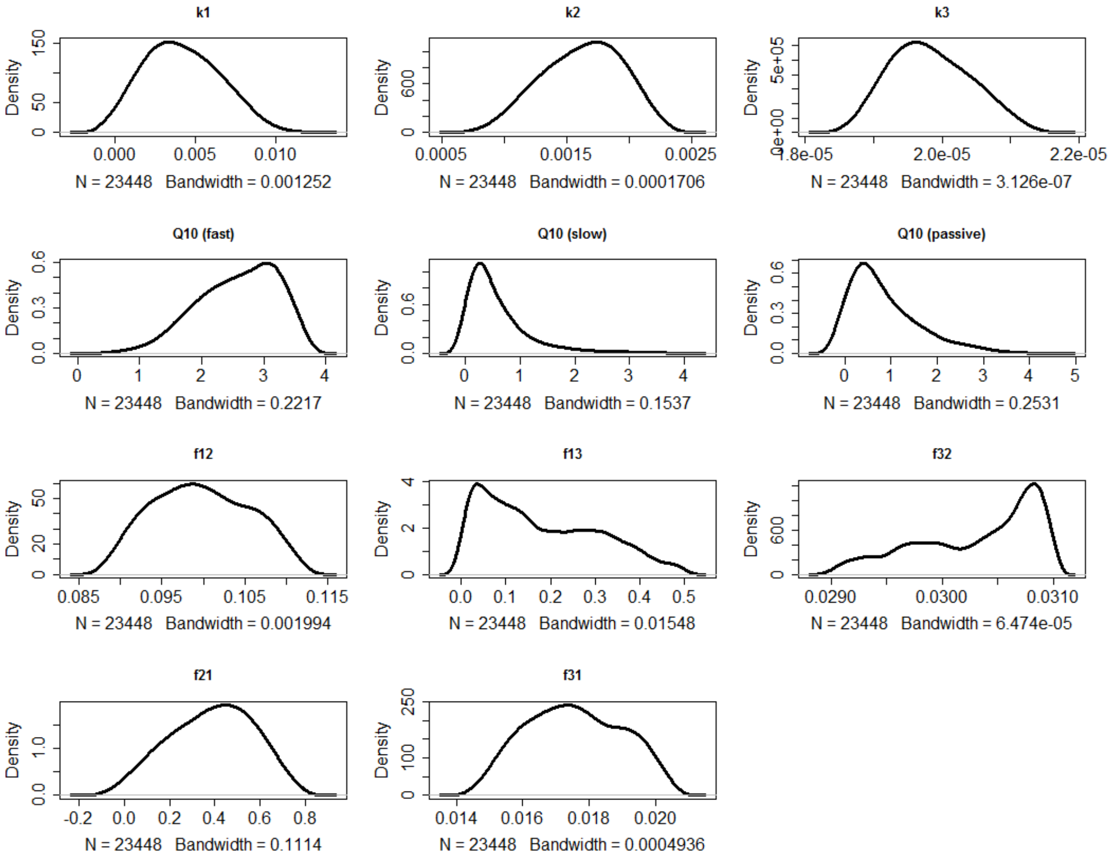

Figure S3. Probability distributions of the parameters in the three-pool model for temperate forest (See Equation (1) for abbreviations).

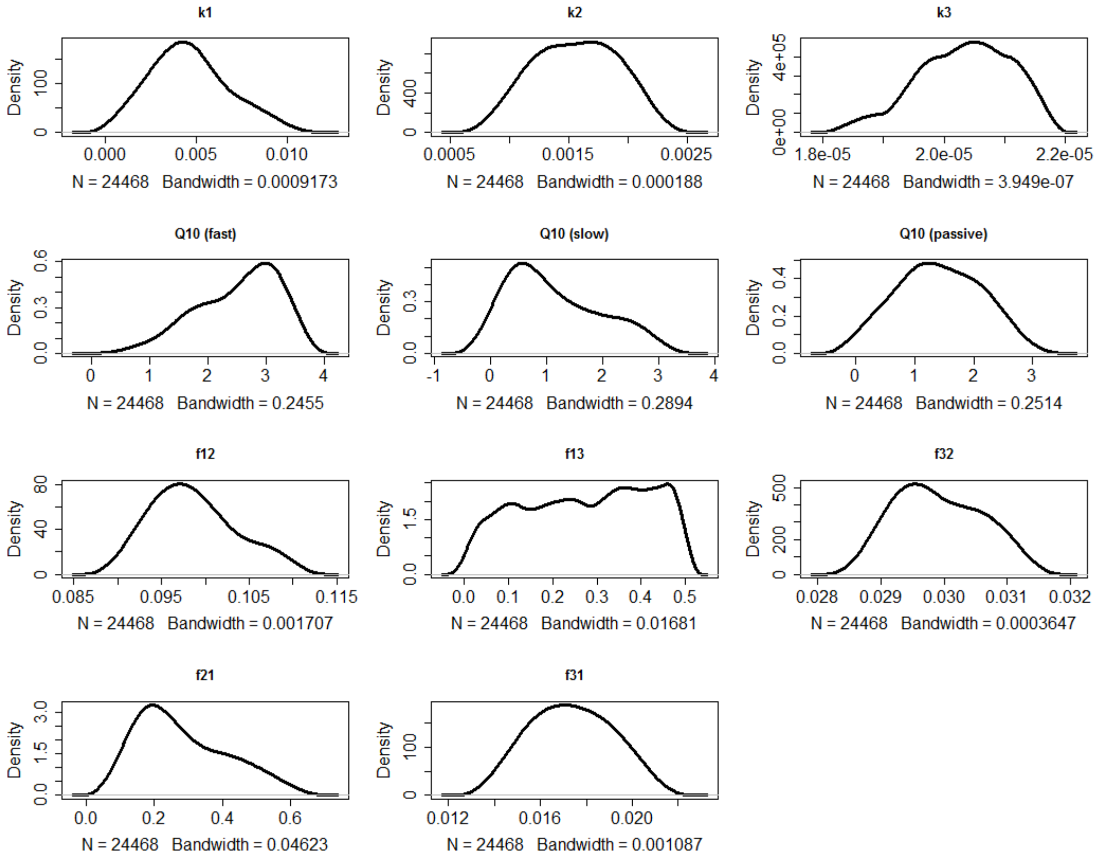

Figure S4. Probability distributions of the parameters in the three-pool model for tropical forest (See Equation (1) for abbreviations).

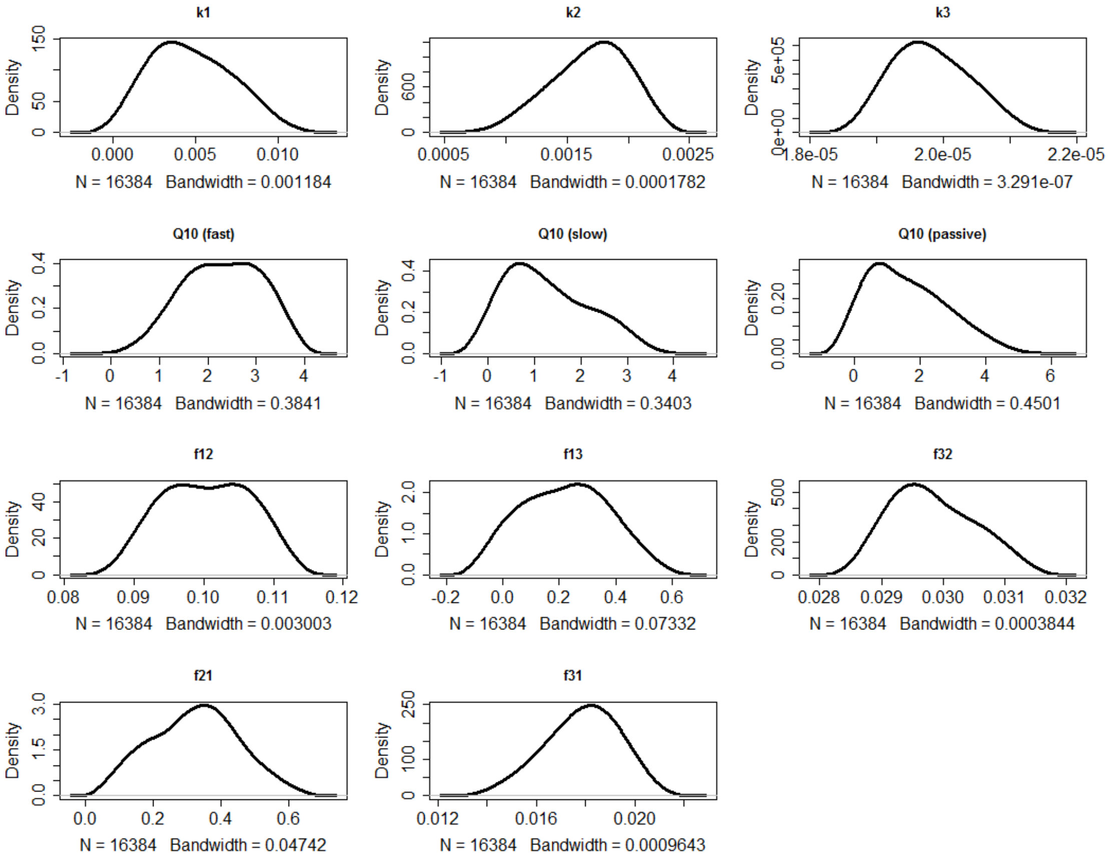

Figure S5. Probability distributions of the parameters in the three-pool model for cropland (See Equation (1) for abbreviations).

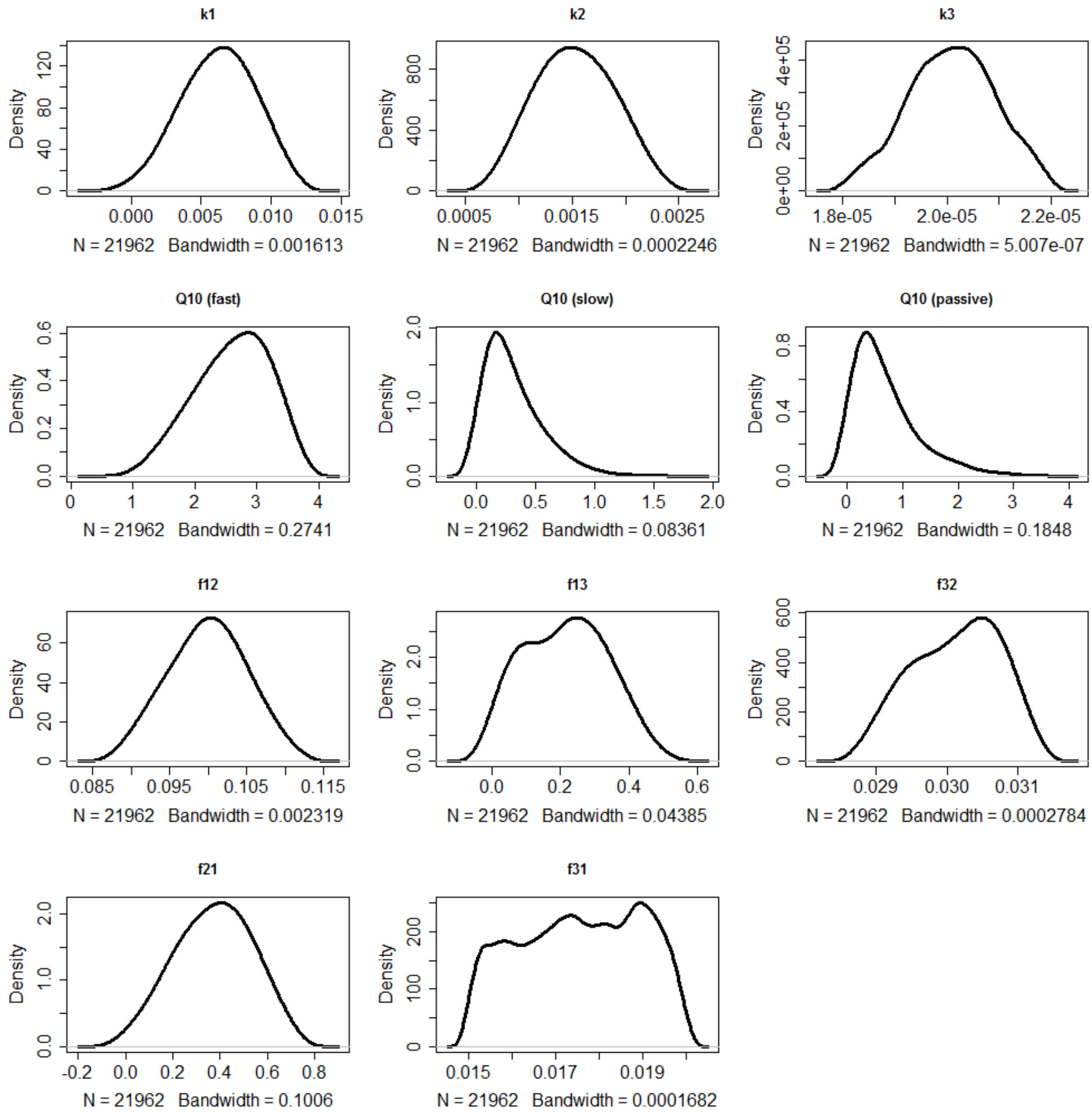

Figure S6. Probability distributions of the parameters in the three-pool model for desert & shrubland (See Equation (1) for abbreviations).

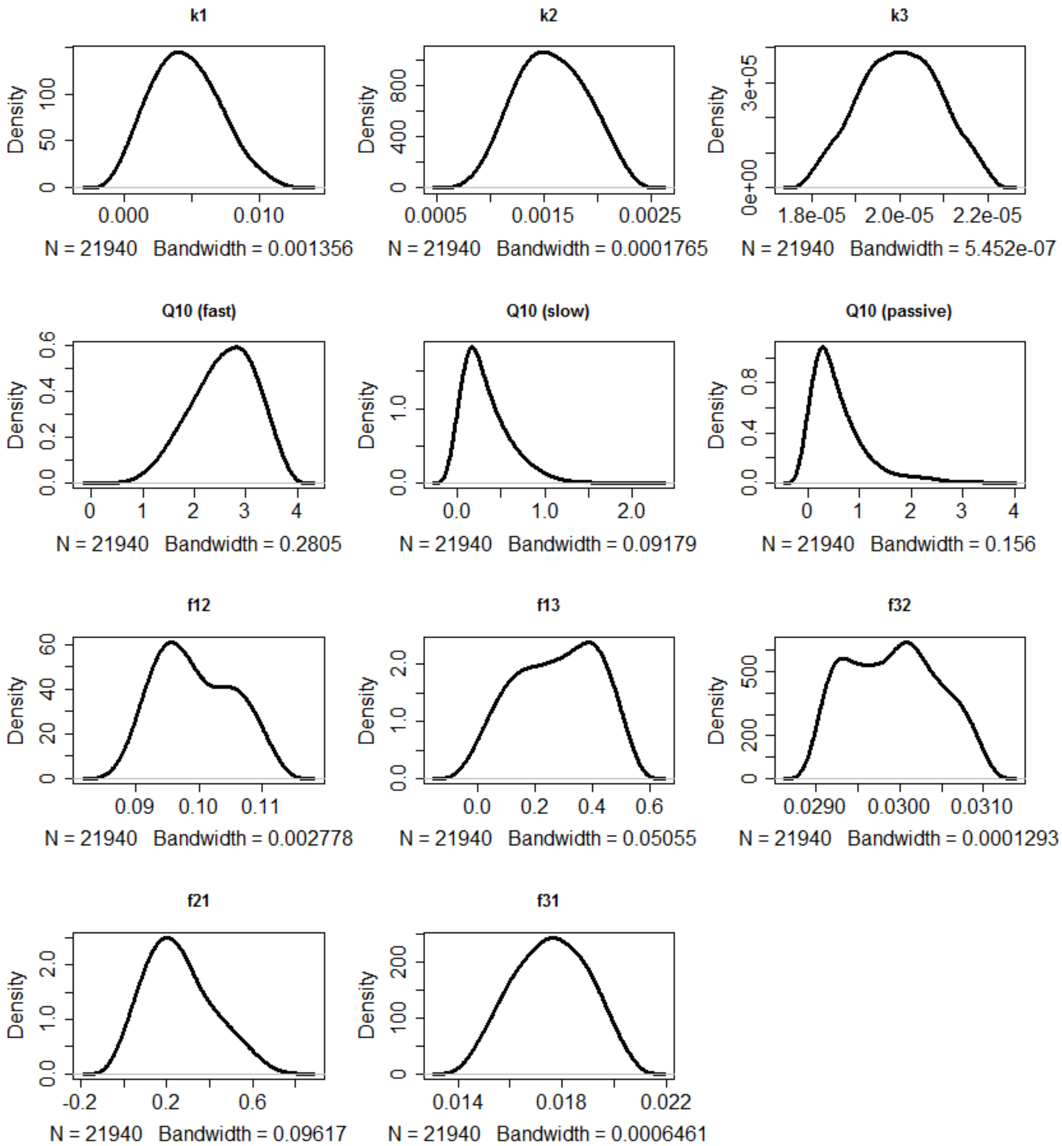

Figure S7. Probability distributions of the parameters in the three-pool model for grassland & savanna (See Equation (1) for abbreviations).